

Stability and interaction of fast auroral solitary structures in three-dimensional plasma

I. Roth, L. Muschietti, C. W. Carlson, and F. S. Mozer

Space Sciences Laboratory, University of California, Berkeley, California, USA

R. E. Ergun

Laboratory for Atmospheric and Space Physics, University of Colorado, Boulder, Colorado, USA

Received 23 May 2001; revised 19 November 2001; accepted 19 November 2001; published 13 September 2002.

[1] The stability of the electrostatic, fast, solitary structures that are observed frequently on auroral field lines is analyzed as a three-dimensional dynamic system and investigated numerically with the help of test-particle and particle-in-cell simulations. The recently observed large-amplitude, localized potential structures with a flat-top shape and separated electric field spikes parallel to the external magnetic field are shown to be supported by a particular self-consistent charge distribution function that differs qualitatively from the distribution that supports the previously investigated Gaussian potentials. The evolution of the solitary structures is related to changes in the trajectories of the supporting, trapped electrons. It is shown that ignoring the interaction with the ions, the planar, isolated spikes propagating into a plasma with realistic, open boundary conditions, are stable in three dimensions. The addition of a perturbation to the large-amplitude primary structure due to a smaller, faster secondary propagating spike results in destruction of the perturbing spike by modifying electron orbits of its trapped population, while the main spike gains an average momentum without any noticeable deformation. The analysis indicates robustness of the solitary spikes on the auroral field lines over significantly long times and their ability to propagate over long distances. *INDEX TERMS*: 2704 Magnetospheric Physics: Auroral phenomena (2407); 2753 Magnetospheric Physics: Numerical modeling; 2772 Magnetospheric Physics: Plasma waves and instabilities; *KEYWORDS*: auroral phenomena, numerical modeling, particle acceleration, electric fields, ionosphere/magnetosphere interactions

Citation: Roth, I., L. Muschietti, C. W. Carlson, F. S. Mozer, and R. E. Ergun, Stability and interaction of fast auroral solitary structures in three-dimensional plasma, *J. Geophys. Res.*, 107(A9), 1239, doi:10.1029/2001JA900175, 2002.

1. Introduction

[2] The observations of solitary structures that move along auroral magnetic field lines constitute one of the recent most interesting magnetospheric discoveries. With the high sampling rate on FAST and Polar satellites it became possible to simultaneously obtain detailed profiles of the spikes as well as a reasonably good distribution functions of the auroral electrons [Mozer *et al.*, 1997; Franz *et al.*, 1998, 2000; Ergun *et al.*, 1998; Carlson *et al.*, 1998; Bounds *et al.*, 1999; Cattell *et al.*, 1999]. The observed spikes move generally in the anti-Earth direction with a velocity the order of the electron thermal velocity spread (1000–5000 km/s), much higher than the ion thermal or drift velocities. These localized, large-amplitude structures are supported by inhomogeneous, nonthermal, trapped electron populations while they modulate the

trajectories of the passing electrons; since the total phase space density is diminished in this region, the solitary structures are inherently related to electron holes. The passing electrons are important indicators of the spikes since they respond instantaneously to any localized electric field and the changes in both the upgoing and downgoing electron fluxes characterize the electromagnetic properties of the spikes. The recent observations at low altitudes (FAST) of solitary structures that move along the auroral magnetic field lines indicate the existence of two different parallel potential profiles for the nonlinear spikes. Generally, the most intense spikes are observed as flat-top potential structures, in contrast to the standard Gaussian-like forms. The perpendicular dimension of both potential forms seem to fill a localized channel across the magnetic field of several kilometers, and the observations indicate a train of solitary pulses with a variety of amplitudes, shapes, and velocities. Similar spikes, although weaker, may have been observed previously in the geomagnetic tail by Geotail [Matsumoto *et al.*, 1994] and in the solar wind by the Wind satellite [Bale *et al.*, 1998]. The

emergence of electron holes from two-stream instability was observed more than 30 years ago [Morse and Nielson, 1969] and with the recent observations was simulated for magnetospheric applications [e.g., Matsumoto et al., 1994; Omura et al., 1996; Miyake et al., 1998, 2000; Goldman et al., 1999; Oppenheim et al., 1999, 2001; Singh et al., 2000, 2001]. Different aspects of their existence and interaction were described by Dupree [1982], Schamel [1982], Turikov [1984], Krasovsky et al. [1997], and others. An important numerical analysis of hole excitation in a linearly stable regime was performed by Berman et al. [1983]; they distinguished between a small “packing fraction” (fractional phase space area occupied by the holes), which describes the system as infrequently interacting solitary structures (similarly to auroral observations), and large packing area, which renders the plasma system as frequently colliding holes with resulting phase space granulations (clumps). Singh and Schunk [1983, 1984] have shown in numerical simulations that some of the electron holes properties may be related to electron shocks. Analytical description of an interaction between electromagnetic waves and charged particles is based on the conservation of phase space density in the absence of external sinks/sources and Coulomb losses. Small deviations from homogeneous equilibrium for particles and external fields are consistent with a neglect of the nonlinear interaction terms, and may be well described by a Fourier spectrum of the excited waves. This description implies periodic modulations of a homogeneous medium due to the propagating waves. The neglected nonlinearity in the interaction terms may result in a development of instability, i.e., fast modification of the wave amplitudes which, eventually, significantly affect the particle distribution functions to make them highly inhomogeneous. Therefore a sufficiently intense perturbation of the homogeneous system requires consideration of the nonlinearity in the lowest-order description, which may result in formation of propagating, inhomogeneous, localized structures. These quasi-stable structures are supported by spatially strongly modified distribution functions, and they are qualitatively different from the linear perturbations. It was shown in the past that a hole describes a most probable self-binding state of maximum entropy [Dupree, 1982; Berman et al., 1985]. Therefore, in many instances the turbulent fluctuations in plasma can be described as a collection of infrequently interacting solitary structures. In contrast to the wavelength-frequency characterization of linear waves, the solitary waves are characterized by their amplitude-shape-velocity relation. Experimental detection of the fast solitary waves requires very high sampling rates, which in the magnetospheric environment were made possible on the latest generation of spacecraft. In this paper we discuss the stability of the nonlinear pulses in three-dimensional environment. The evolution of a specific spike depends on the adjustment of the trapped population to perturbations and to externally modified parameters. The strongest perturbations that affect a solitary spike may be due to its interaction with other spikes moving relatively to it; when two spikes approach each other, the supporting electron distributions intermingle and their mixture may cause a destruction or deformation of the spike(s). Therefore evolution and interaction of solitary

structure(s) may be described well with the help of motion of particles whose strongly perturbed trajectories support the structure. Section 2 presents the characterization of the propagating auroral potential structures, section 3 analyzes the test particle phase space dynamics in the given potential structures, and section 4 describes the results of self-consistent particle-in-cell (PIC) simulations with open boundaries of isolated and interacting spikes.

2. Parametrization of the Potential Structures

[3] In several cases of the previously published fast propagating auroral potential structures, a Gaussian or bi-exponential function gave a reasonably good fit to the measured potential forms. In this potential form the (measured) parallel electric field is seen as adjacent reversed spikes [Mozer et al., 1997; Ergun et al., 1998] and the self-consistent electron density has a deficiency of electrons in the central part of the electron hole with a surplus at its edges [e.g., Muschietti et al., 1999]. However, in numerous cases, as shown in Figure 1, a more appropriate description would depict the potential along the parallel coordinate (ambient magnetic field) as a quasi-symmetric function with a flat-top and a sharp decline at the edges. One may observe a series of pulses where generally the perpendicular field is unipolar while the parallel field exhibits two bipolar spikes, frequently separated by a region of a constant potential (null electric field). The structure of each spike, as it encounters the satellite, is reflected by the measured electron fluxes. The passage of the solitary structure affects the upgoing (top panels) and downgoing (bottom panels) electrons by shifting their distribution function, as can be seen by the changing colors of the most intense energy fluxes. The electrons carry all the field information integrated over their trajectories; therefore the changing colors of increased fluxes towards higher energies apply to both the upgoing and downgoing electrons that are accelerated by the separate electric field regions of the flat-top or Gaussian potential. To prepare for future analyses of the interaction between two spikes, we model their combined potential in a separable form as

$$\Phi(x, r) = \phi_0 G_o(x) R_o(r) + \phi_1 G_1(x) R_1(r), \quad (1)$$

where x denotes the axial, parallel coordinate, $r^2 = (y^2 + z^2)$ is the perpendicular radial coordinate, and the indices o and 1 denote the primary and the secondary spikes, respectively. The parallel dependence of the recently observed potential structures is described by the symmetric flat-top function

$$\begin{aligned} G_o(x) &= [1 + \exp(-d/\Delta_x) \cosh(x/\Delta_x)]^{-1} \\ &= \{1 + 0.5(\exp((x-d)/\Delta_x) \\ &\quad + \exp((-x-d)/\Delta_x))\}^{-1}, \end{aligned}$$

while the previously analyzed Gaussian potential is described by

$$G_o(x) = \exp[-x^2/\Delta_x^2].$$

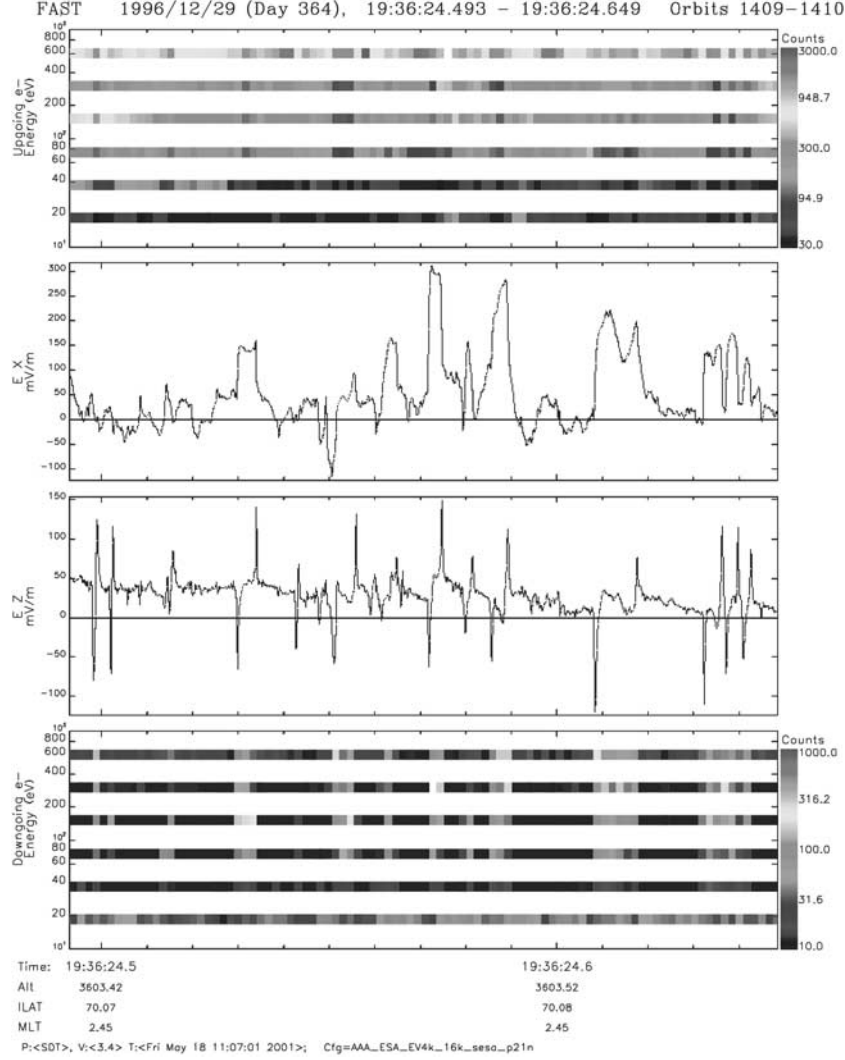


Figure 1. Energy fluxes at several energy channels for (top) upgoing and (bottom) downgoing electrons. (middle, top) Perpendicular and (middle, bottom) parallel electric field components with flat-top and Gaussian solitary structures. See color version of this figure at back of this issue.

Owing to insufficient details in the single spacecraft measurements, the perpendicular form factor is taken as a Gaussian

$$R_o(r) = \exp[-r^2/\Delta_r^2]$$

The parameters d and $\Delta_x = \Delta_{\parallel}$ denote, respectively, the “width” of the flat-top structure and the width of the bipolar electric field region along the external field, while $\Delta_r = \Delta_{\perp}$ describes the scale length perpendicular to the external field. By increasing the relative ratio between d and Δ_x one can shift from a form resembling a bi-exponential ($d \ll \Delta_x$), which differs only slightly from the Gaussian-like structure, to a proper flat-top shape ($d \gg \Delta_x$). Figure 2 shows the deformation of the potential structure for an arbitrary amplitude of $\Phi_0 = 10$, as d takes the values 1, 2, and 4, while $\Delta_x = 1.3$. Experimentally, the extended flat-top potential is deduced from the observed parallel electric

fields. The existence of this form requires a particular charge density that supports the potential structures. Since the solitary structure exhibits a positive potential, the supporting trapped distribution has deficiency of electrons at its center; i.e., it contains an “electron hole.” Figure 3 shows again a cut for $R = \text{const}$ of the flat-top potential, together with the resulting well-separated, parallel bipolar electric field components, as well as the (unnormalized) self-consistent modification to the electron charge density. The electric field in Figure 3b resembles some of the experimentally measured parallel field forms in Figure 1, while the potential structure of Figure 3a is supported by a self-consistent, phase space distribution function that produces the distorted charge density of Figure 3c. This excess charge density is qualitatively different in the central part of the hole from a charge density which is consistent with the Gaussian potential [e.g., Muschietti *et al.*, 1999]. The Gaussian potential does not require the “bulge” for the charge density in its center. The net charge density of the inhomogeneous

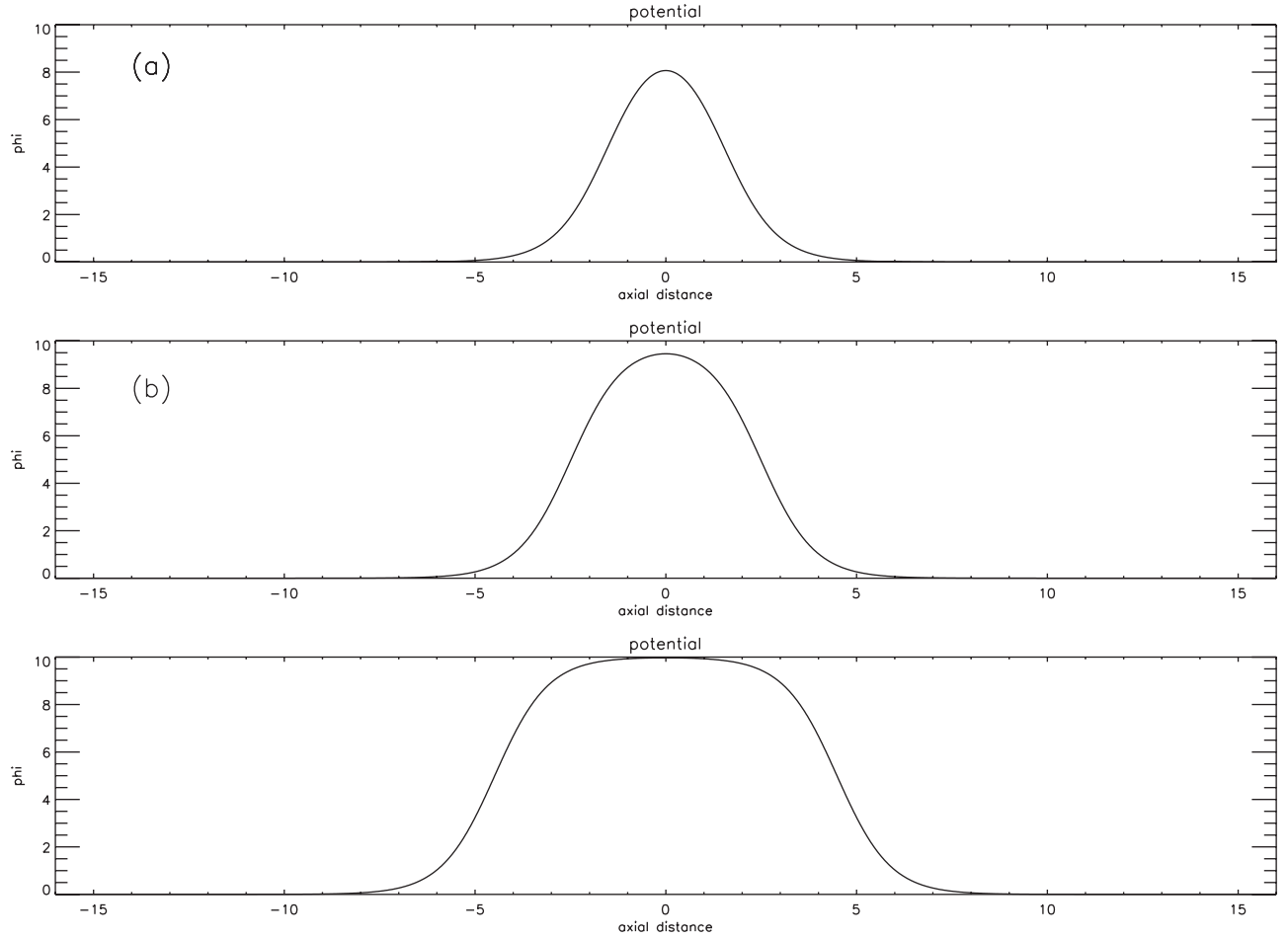


Figure 2. The unnormalized potential structure as a function of the parallel coordinate effect of varying the flat-top region d : (a) $d = 1$, (b) $d = 2$, and (c) $d = 4$; the other parameters are $\Delta_x = 1.3$ and $\Phi_0 = 10$.

spike is produced by the trapped particles that support the structure and the passing particles that are deflected by the potential structure. A qualitative difference in the distribution functions that support the flat-top and the bi-exponential/Gaussian potentials, respectively, stems from the fact that the passing particles are accelerated by the electric force of the spike, so their density decreases [Muschiatti *et al.*, 2002]. In the central region of the flat-top (constant) potential this decreased charge must be compensated by additional trapped electrons; thus this deficit results in the central bump in the trapped population. In the Gaussian case this region of constant potential is of measure zero, hence no increased density of trapped electrons (bulge) in the center of the hole is required. Figure 4 shows the two-dimensional contours of a potential $\Phi(x, r)$ as described by the first term of equation (1), together with the contours of a self-consistent density. One observes the electron hole in the central part of the spike, a surplus of electrons at the edges, and decreasing contour levels with increasing radial distance. The cut along the line $r = 0$ is equivalent to Figure 3c. Since the potential decreases with increasing radial distance r , both the absolute value of the charge density and the relative bulge in the center of the spike diminish with r . The second term in equation (1) describes the nonnegligible potential perturbation of the main

solitary structure, which is due to a secondary spike approaching the main structure. We simplify it as

$$G_1(x) = \exp\left[-(x - x_1)^2/\delta_x^2\right]$$

$$R_1(r) = \exp\left[-(y^2 + z^2)/\delta_r^2\right],$$

where $x_1(t)$ denotes the relative distance between the approaching spikes. As the spikes approach each other, the amplitudes ϕ_0 and ϕ_1 and the form factors $G_i(x)$, $R_i(r)$, for $i = 0, 1$, determine the deformation of the electron phase space densities. These deformations determine the stability and evolution of the spikes. Generally, we assume $\phi_0 > \phi_1$.

3. Dynamics of the Trapped Electrons

[4] Since the stability of the potential structure is inherently related to the phase space motion of the trapped particles, any possible coupling between the different constants of motion or their violation in a presence of external perturbation is of major importance. In order to analyze the stability of the spikes and the effect of external perturbations on the trajectories of the trapped, magnetized electrons, support the three-dimensional potential structures, we

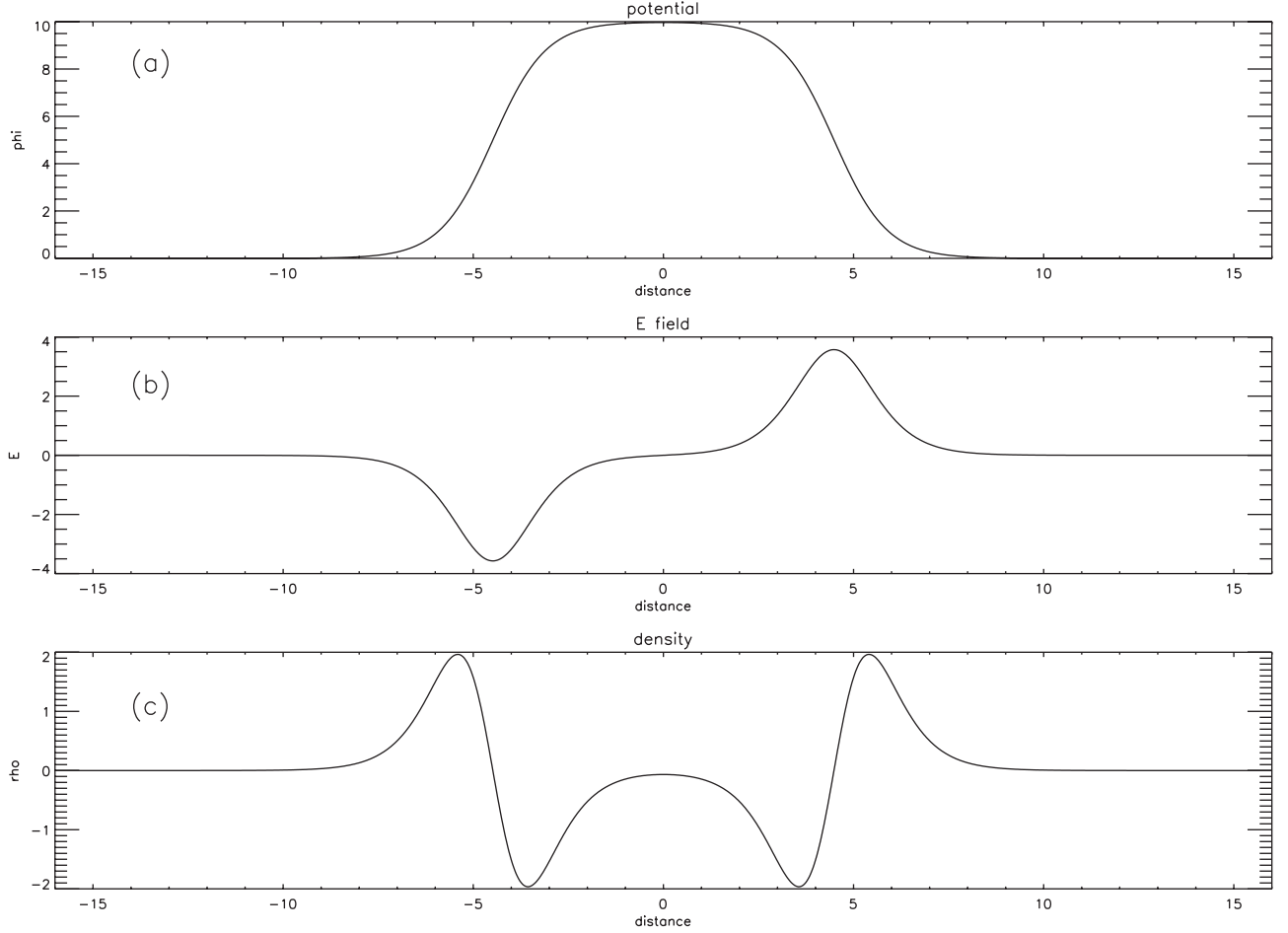


Figure 3. Model of (a) potential structure, (b) parallel electric field, and (c) self-consistent modifications to charge density as a function of the parallel coordinate: $d = 4$ and $\Delta_x = 1.3$. The amplitude is chosen arbitrarily as $\Phi_0 = 10$, which scales accordingly all other quantities.

impose given external fields, as derived from equation (1), and follow representative electrons in phase space to discern the changes in their orbits under different external conditions. For each particle we propagate in time a six-dimen-

sional vector that describes its phase space: $\mathbf{X} = (x, y, z, v_x, v_y, v_z)$. The set of the coupled equations

$$\dot{\mathbf{X}} = \mathbf{H}(\mathbf{X}), \quad (2)$$

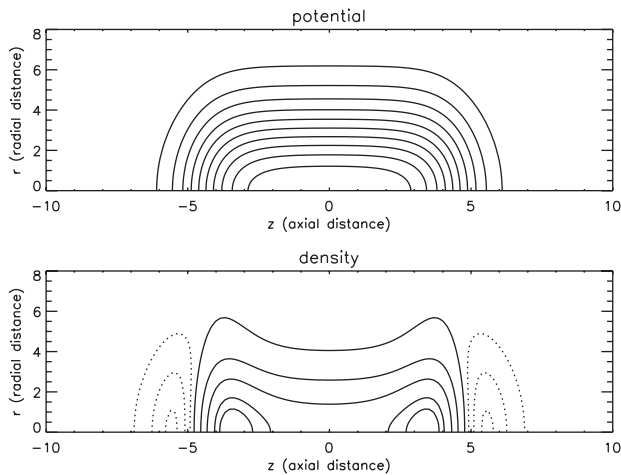


Figure 4. Two-dimensional contours of the potential $\Phi(x, r)$ and the self-consistent charge density $\rho(x, r)$. $\Delta_x = 0.7$, $\Delta_r = 4$, and $d = 4$. The solid and dashed lines represent negative and positive contour levels, respectively.

where the vector \mathbf{H} describes the changes in the phase space dynamics via the prescribed electromagnetic fields (external constant magnetic field and electric field derived from equation (1), is solved with an adaptive time step. The normalization describes the time in units of inverse gyrofrequency and distances in Debye lengths. The results are displayed as a time series of a specific phase space variable (coordinate or velocity component) or two-dimensional projection of the phase diagram. Due to the structure of the electromagnetic forces, equation (2) describes an autonomous (no explicit time dependence on the right-hand side of the equation) and conservative (volume preserving, i.e., $\nabla \mathbf{H} = 0$) system. In Figure 5 we show the time series oscillations of the perpendicular y and z positions, parallel position and velocity, for a low-energy electron (kinetic energy \ll maximum potential energy of the spike) in the presence of a three-dimensional flat-top potential with $\Delta_r = d \gg \Delta_x$. For this low kinetic energy the bounce motion of the electron is similar to a modified linear harmonic oscillator, as can be observed in the bounce oscillatory structure of the parallel motion (two bottom figures), in the

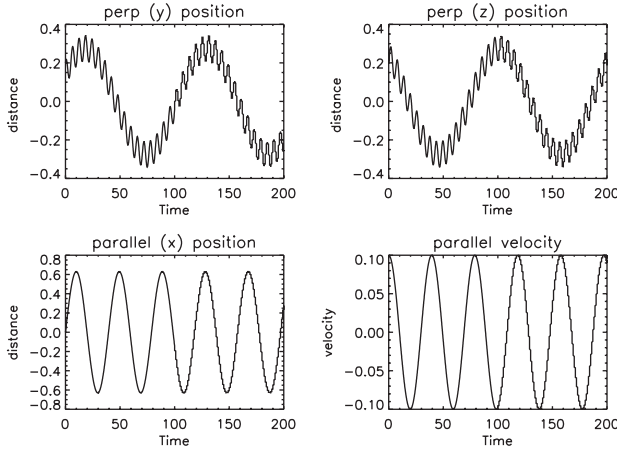


Figure 5. Temporal phase space variables for a low-energy trapped electrons in the presence of a single spike: perpendicular y position, perpendicular z position, parallel position, and parallel velocity. $\Delta_x = 1.3$, $\Delta_r = 4$, $d = 1.3$, $\phi_0 = 0.56$, and $v_{||} = 0.1$.

fast gyration around the magnetic field and an average slow drift across the magnetic field in the perpendicular coordinates (two top figures). Figure 6 shows, for the same parameters, the phase space evolution of (1) the perpendicular coordinate with time, (2) the perpendicular coordinates projection of the phase space, (3) the deformed oscillation in the parallel velocity, and (4) the parallel phase space projection for an electron close to the separatrix with the initial values: $v_{\perp} = 0.07$, $v_{||} = 1.38$. One observes a slight modification of the gyration-drift motion (two top figures), and deformation of the parallel trajectories in the flat-top potential region with increasing electron energies (bottom figures). Owing to the strong magnetization on the auroral field lines and the small perpendicular thermal spread, the gyroradius is much smaller than any perpendicular gradient of the spike's potential, and only weak coupling between parallel and perpendicular oscillations occurs. The self-

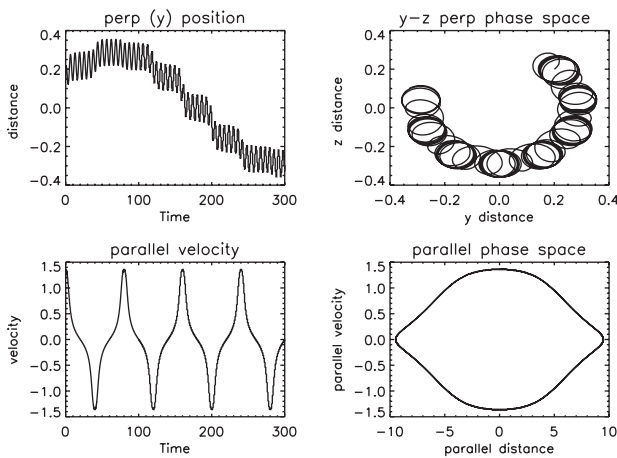


Figure 6. Cuts in phase space variables in the presence of a single spike for an electron close to the separatrix: perpendicular (y) coordinate versus time, perpendicular coordinates phase space, parallel velocity versus time and parallel phase space. $\Delta_x = 1.3$, $\Delta_r = 4.0$, $d = 4.0$, and $\phi_0 = 1.0$. Initial conditions: $x = 0.0$, $v_x = 1.38$, and $v_y = v_z = 0.05$.

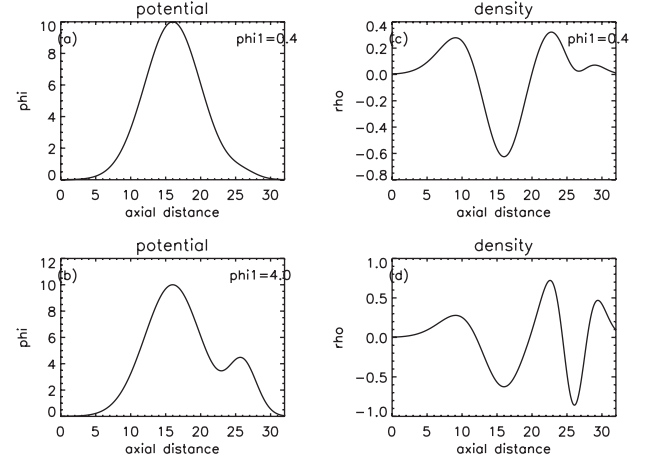


Figure 7. One-dimensional projection of the potential and the density along the parallel axis in the presence of a main solitary structure and a secondary spike. The unnormalized amplitude of the spikes are $\phi_0 = 10.0$ in all panels, $\phi_1 = 0.4$ in Figures 7a and 7c, and $\phi_1 = 4.0$ in Figures 7b and 7d.

consistent evolution and stability of a spike will be shown with the help of PIC simulations in the next section; it can be approximately analyzed with the help of the trajectories of the trapped electrons in the presence of a spike having a substantial perturbation. Since the observations indicate a stream of spikes filling a channel along specific field lines, the most natural perturbation to the self-consistent spike may be described by another solitary structure which is slowly approaching the main spike. When the two spikes are sufficiently close, such that the distance between their centers is of the order of the sum of the parallel gradient scales of the respective potential structures, the more energetic trapped electrons, close to the separatrix, may tunnel out between the two structures. In this event a simple analytical description for the potential may be given by equation (1) with the inclusion of the second term. Figure 7 shows the projection on the parallel axis of the potential and the resulting density. Figures 7a and 7c refer to the amplitude ratio $\phi_1/\phi_0 = 0.04$ while Figures 7b and 7d show it for the ratio of 0.4. One may conclude that the trapped particles in the main spike close to the separatrix and below it may easily penetrate into the other spike. Since the existence of a spike depends sensitively on the structure of the trapped particles, and the phase space density of the primary spike particles near the separatrix is much larger than in the smaller perturbing spike, the net injection of electrons into the secondary spike adds the “missing” charge of the electron hole leading to a possible disappearance of the smaller, secondary hole and its potential spike. Figure 8 shows the phase space cuts from test particle phase space trajectories, similarly to Figure 6, in the presence of the two spikes with amplitude ratio $\phi_1/\phi_0 = 0.4$. One observes significant perpendicular deviations (in velocities and positions) for the electron at the separatrix, with a major perturbation in the parallel phase space as the electron penetrates from the main solitary structure to the secondary spike. The electrons are still tied to the field lines, as can be observed from the perpendicular projections of the phase space trajectory (Figure 8c), the drift and gyration can be clearly identified and the perpendicular velocity which fills a ring for low

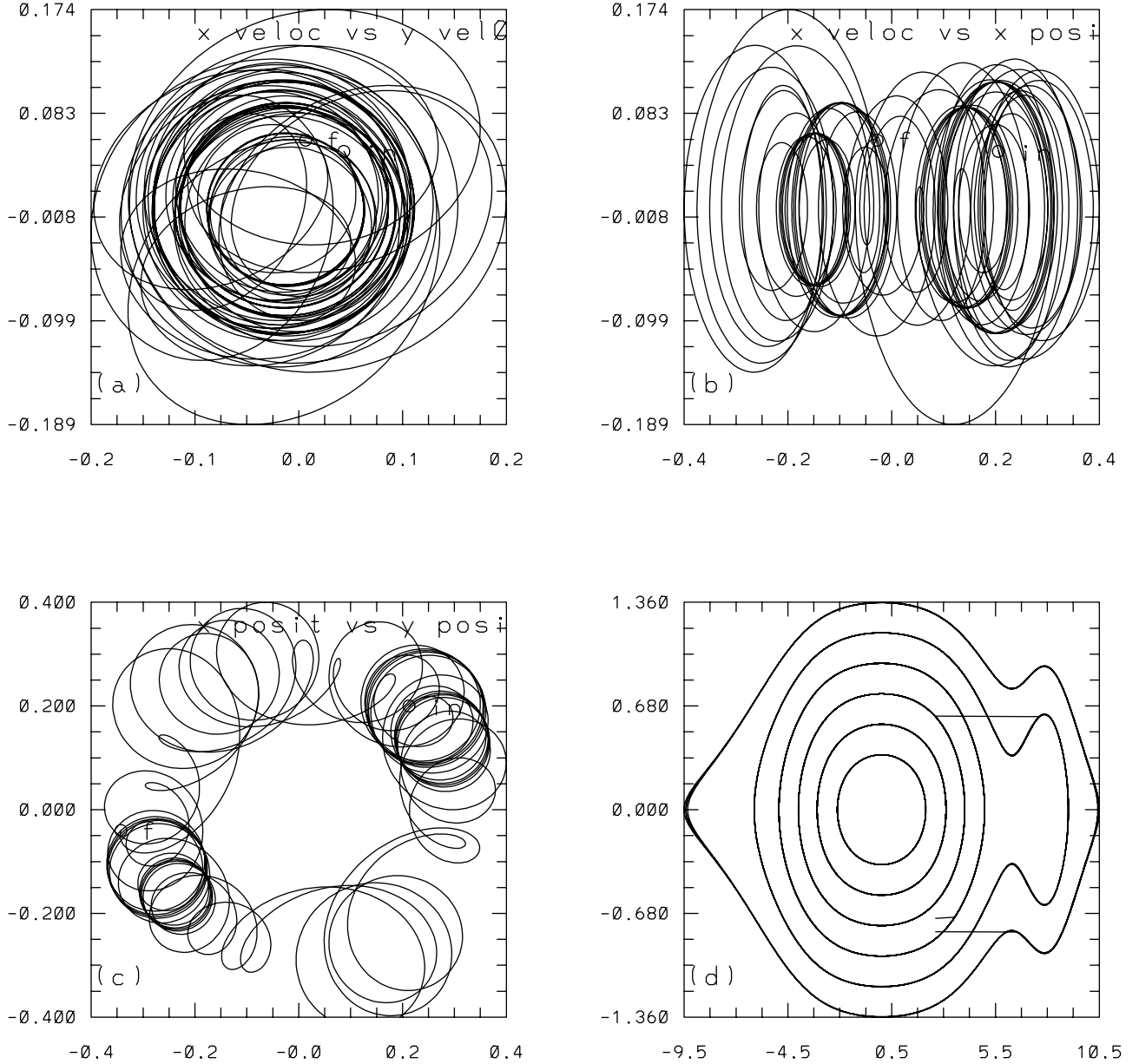


Figure 8. Phase space cuts in the presence of a primary (o) and secondary (l) potential spike for $\phi_0 = 1.0$ and $\phi_1 = 0.4$. Parameters of the principal spike are $d = 4$, $\Delta_x = 1.3$, and $\Delta_r = 4$. Parameters of the secondary spike are $\delta_x = 1.0$ and $\delta_r = 1.0$. The distance between the spikes $x_1 = 8.0$. The plots show (left to right, top to bottom) the following: (a) two perpendicular velocities, (b) perpendicular velocity versus perpendicular position, (c) two perpendicular positions, (d) parallel velocity versus parallel position for several electrons. Initial conditions in Figure 8a–8c: $x = 0.2$, $y = 0.2$, $z = 0.0$, $v_{||} = 1.36$, $v_y = 0.05$, and $v_z = 0.05$. In Figure 8d, $v_{||}$ are spread linearly from $v_{||} = 0.36$ to 1.36 .

energy electron gets smeared; in contrast, the parallel oscillation is greatly modified for the electrons near the separatrix. This modification is responsible for the short lifetime of the secondary spike, as will be shown in the next section.

4. Self-Consistent Interaction Between Two Spikes

[5] The emergence of turbulence in a plasma from a quiescent, linearly stable state was investigated in one-dimensional simulations by *Berman et al.* [1983, 1985]. It

was shown that an isolated hole can grow for any finite drift between electrons and ions. The interaction between two holes was described by *Dupree* [1982] with the help of entropy considerations; coalescence of holes diminishes the electric field energy by accelerating the plasma particles that support the emerging solitary structure. Here we detail the processes of the emerging structure as seen by the trapped population of electrons and their dynamics in a presence of a significant perturbation as described by a secondary solitary structure. Previous particle-in-cell simulations for auroral applications indicated that an isolated one- or two-dimensional spike is very robust over many plasma periods

in the presence of a strong magnetic field [e.g., *Muschiatti et al.*, 2000]. In order to validate the stability of the solitary structures in more realistic conditions, we extended our code to allow simulation of the nonlinear structures in three-dimensional environment. All the particle and field/potential quantities are functions of x, y, z , where x denotes the coordinate along the external field line. It is assumed that a potential profile made out of one or more spikes with specific characteristics has been formed and coexists with the populations of trapped and passing electrons. We follow the evolution of the potential as determined by the full dynamics of the particles in an open-boundary, self-consistent, electrostatic PIC code. The solitary structures are created from the constants of motion for the particles that move in phase space under the influence of the structure [*Muschiatti et al.*, 1999, 2002]. The trajectories of the particles depend on the amplitude and the shape of the solitary structure. The resulting distribution function is spatially inhomogeneous with trapped and passing particles, depending on their energies. In these simulations the boundary conditions along the external field line allow any given external flux of particles to enter with an arbitrary distribution function, while those particles that leave the system are lost and ignored. The resulting total number of particles fluctuates in time, causing a (realistic) small fluctuation of the potential on the right boundary (the left boundary is kept at zero value). In the present simulations we choose for the impinging particles at the boundary either a one-sided Maxwellian, with or without a tail (similarly to a κ function). The time-varying potential at the right boundary is obtained from integration of the parallel current over all the field lines on the numerical grid. This self-consistent, time-varying boundary condition is close to realistic, although the small size of our system may suppress eigenmodes that may be responsible for long time evolution of the spikes; it differs from many of the other boundary conditions implemented in auroral simulations [*Omura et al.*, 1996; *Miyake et al.*, 1998, 2000; *Goldman et al.*, 1999; *Singh et al.*, 2000, 2001; *Crumley et al.*, 2001; *Oppenheim et al.*, 1999, 2001]. Generally, the timescales for the evolution of the solitary structures are hundreds or thousands of times longer than the crossing time of an electron through a solitary structure. Large systems, with open or periodic boundary conditions, allow for an excitation of additional eigenmodes that may be important in the long-term evolution of the structures; however, for an investigation of an isolated structure or a pair of solitary structures a repeated circulation of the same electrons in periodic simulations may inject artificial effects. Additionally, open system does not necessarily conserve the total momentum of a spike, which can be exchanged with the external environment by the nonthermal electrons that are emitted through the open boundaries. This allows deformation and acceleration of the solitary structures that may be of importance in the evolution of interacting spikes. The simulation is carried out in the frame of one of the potential spikes so as to follow the evolution over long times without the spike moving out of the simulation box. Because we concentrate on the evolution of an isolated spike, or interaction between two spikes at a close range, we do not require long systems. Therefore, with a few million of particles on a grid of $32 \times 32 \times 32$ we obtain an excellent spatial particle resolution of $>100/\lambda_D^3$. Since

comparison runs with mobile and stationary ions showed no effects over the simulation timescales, in the present set of simulations the ions are taken as immobile, i.e., homogeneous and constant to neutralize the electrons in a time average sense. Over longer simulation times it was shown that the system of solitary structures may decay via emission of electrostatic whistler waves [*Oppenheim et al.*, 1999; *Singh et al.*, 2000, 2001]. For the perpendicular dimension we apply periodic boundary conditions, which are well justified for the strongly magnetized plasma with small gyroradii. In the runs presented, the cyclotron frequency is varied with respect to the plasma frequency in the range $\Omega_e = 1 - 5 \omega_e$. Since we are not interested in the effect of the solitary perpendicular field on the ions, we start with a primary planar Gaussian or flat-top solitary structure and a smaller but finite amplitude perturbation in the form of a secondary spike. We display interchangeably representative results from both Gaussian and flat-top simulations with similar conclusions relating to stability and evolution of the spike(s). The initial distributions are constructed by the method described by *Muschiatti et al.* [1999, 2002]. Figure 9 shows the evolved single potential structure which was initiated similarly to that in Figure 3, after 200 time steps, each of $0.2 \omega_p^{-1}$. The bottom of Figure 9 displays the two-dimensional projection contours, $\phi(x, y)$, of the three-dimensional potential $\phi(x, y, z)$ at a given value z . The top of the Figure makes cuts of $\phi(x)$ for three values of y as noted. The stability of the potential form is preserved for thousands of time steps (hundreds of electron and about tens of ion plasma periods, respectively). Figure 10 depicts similar contour plots for the charge density, which is noisier than the potential of Figure 9 because charge density is obtained from single particles while the potential results from an integration that smooths its features. Nevertheless, Figure 10 (top) resembles the charge density of Figure 3c. In the next set of runs we test the behavior of the primary spike when it is perturbed by a second, less intense, approaching spike. We create a primary, self-consistent Gaussian (in the parallel direction) spike and adiabatically add an additional spike that moves very slowly towards the main investigated solitary structure (i.e., it approaches it while both of them are moving along the auroral field lines), while its amplitude is increased slowly to allow the trapped particles in phase space to adjust themselves to the total potential. Specifically, we ramp up slowly the amplitude of the secondary spike while changing its central location; inspection of the phase space indicates a small hole dug out by the secondary potential. When the second spike reaches a sufficiently large amplitude ($\phi_1/\phi_0 = 0.4$) and approaches the main structure within the parallel scale lengths (Figure 11) at the time $40\omega_p^{-1}$, self-consistently. We observe that after a short time (less than 25 plasma periods) the smaller, perturbing spike disappears almost entirely, while the main spike gets a small boost in the direction of the motion of the perturbing spike. This destruction (cannibalism) of the secondary spike is due to the phase space modifications in the trapped electrons. The electrons that support the main solitary structure, with a much higher density around its separatrix than those that support the (smaller) secondary spike, gain access to the secondary spike and, in a very short time, cause a major disruption of the delicate phase space configuration which supports the spike. As they enter the secondary spike, they

3D - FatSW

step= 200 time= 40.00 potential(x,y) at z=8

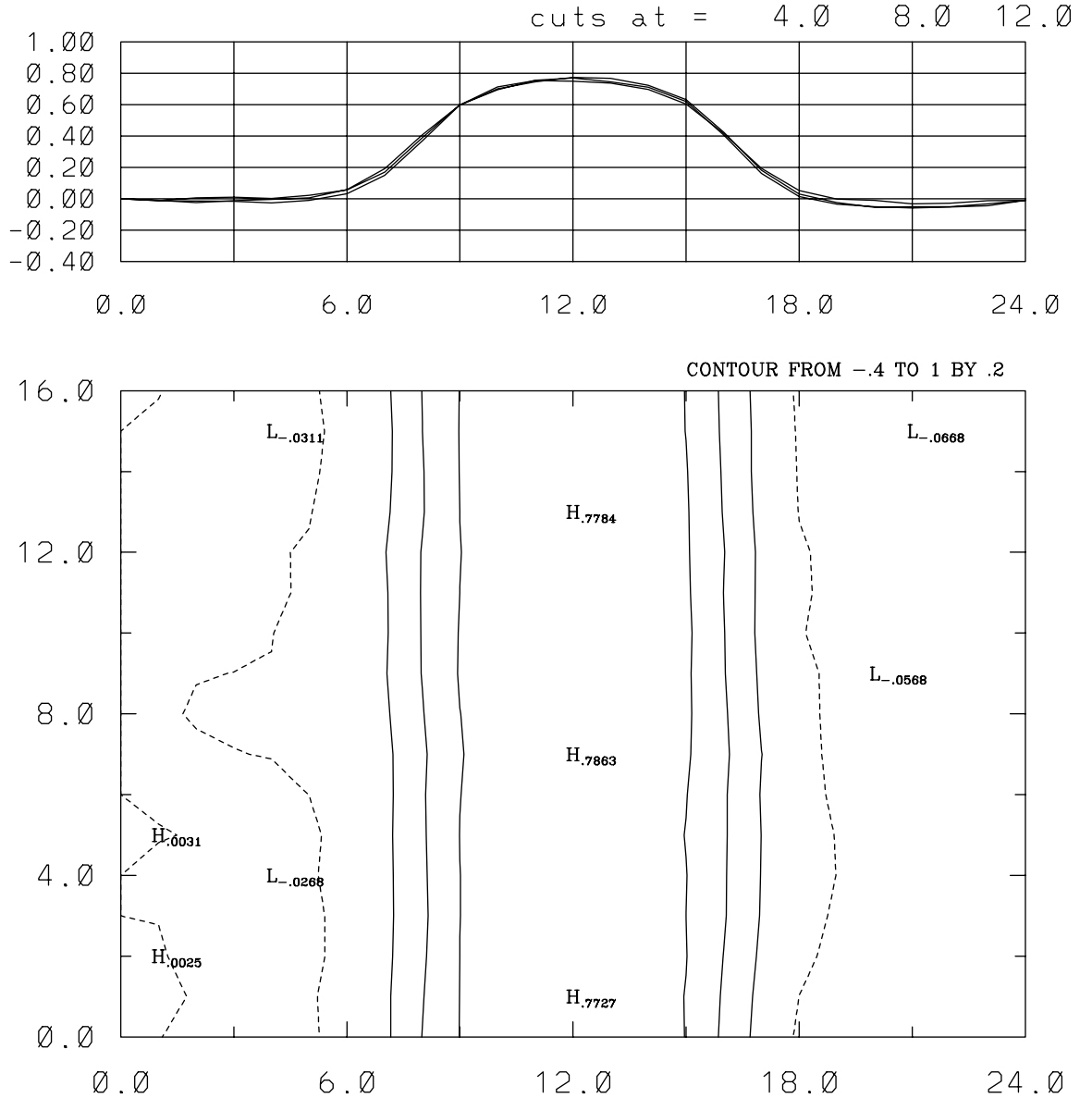


Figure 9. Two-dimensional projection of the flat-top potential $\phi(x, y)$ for $z = L_z/2$ and cuts $\phi(x)$ for three y values after 200 time steps. All the dimensions are given in Debye lengths. $\Omega_e = 2 \omega_e$. The right boundary fluctuates due to the external influx of particles causing the small flapping of the potential at this boundary. The structure indicates robustness.

“fill” its electron hole. Because the electrostatic potential structure responds rapidly to the changes in phase space, the new electrons decrease the electron hole, the spike diminishes and the injected electrons become untrapped (passing electrons for the diminished secondary spike). This description complements the test particle analysis of Figure 8, which did not consider the feedback of the electrons on the potential structures. As a result of this strong phase space deformation of the supporting and passing electrons, the secondary spike cannot sustain its shape. Additionally, those electrons which were trapped originally in the

primary spike close to the separatrix and that became passing electrons with the demise of the secondary spike, carry with them significant momentum. Since this momentum was originally part of the primary spike, and there is no such loss of momentum of trapped particles moving in the other direction, the main solitary structure starts moving in the opposite direction. Figures 12 and 13 depict the potential structure, in a format similar to that of Figures 9 and 11, at later simulation times. One observes almost a complete disappearance of the secondary spike and an average drift of the main spike opposite to the original

3D - FatSW

step= 200 time= 40.00 el. charge(x,y) at z=8

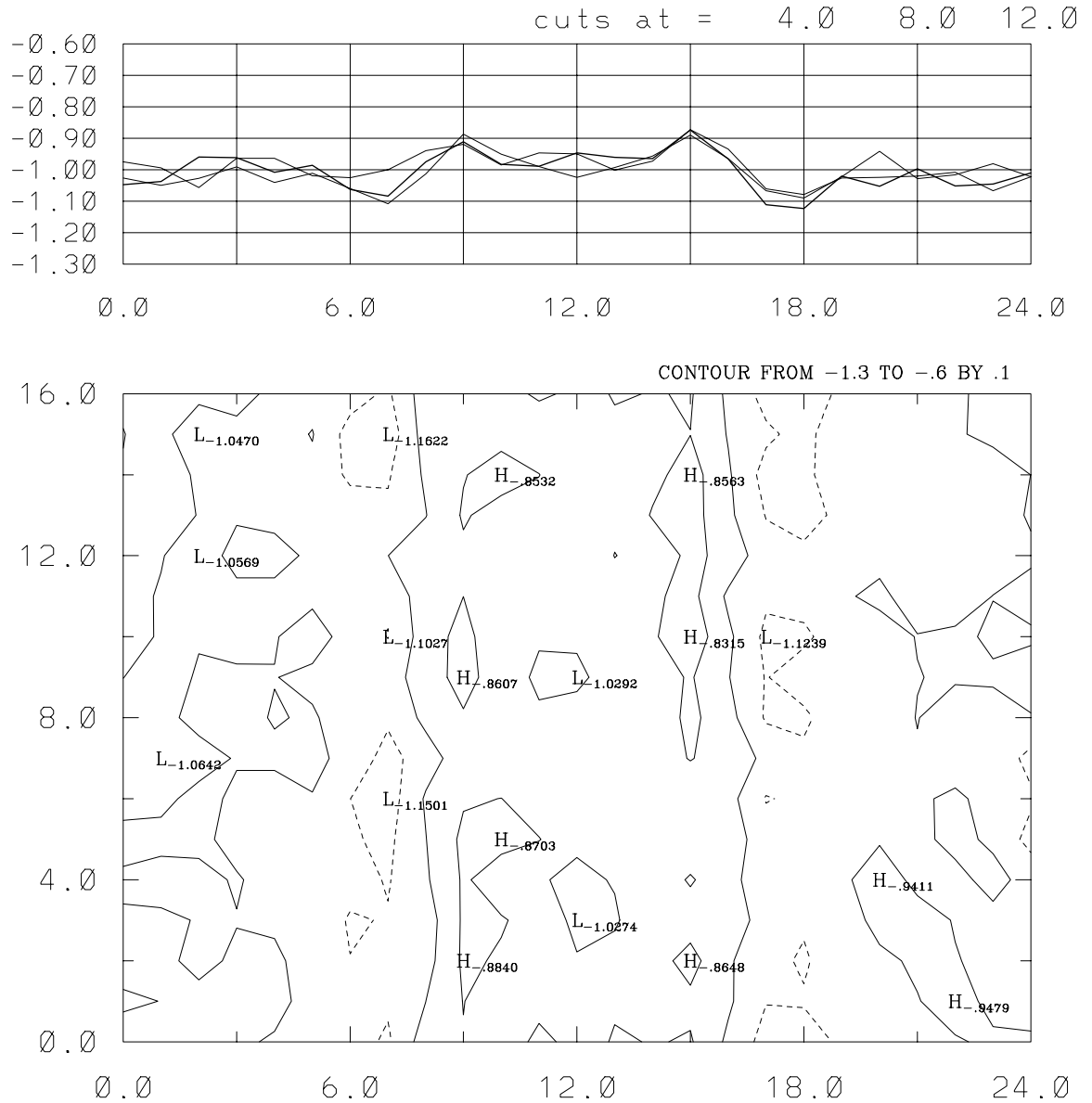


Figure 10. Two-dimensional projection of the self-consistent charge density $\rho(x, y)$ for $z = L_z/2$ and cuts $\rho(x)$ for three y values. Note the reverse scale at the top.

location of the secondary spike. Therefore the interaction between spikes may be a source of the destruction of the less-intense spike; additionally, the interaction may accelerate or decelerate some of the fast, more intense solitary structures. This may be an additional source of variety of speeds in the observed spikes.

5. Discussion and Summary

[6] The fast, intense, magnetized solitary structures which propagate along the auroral field lines display a long time stability. Most of the spike profiles can fit parallel Gaussians, but some of the more intense spikes exhibit flat-top parallel

potential structures with strong perpendicular fields. These two solitary structures with different profiles are supported by different self-consistent charge densities. The flat-top potential requires an enhanced, trapped electron population that compensates for the decreased population of passing electrons along the flat-top domain. For a Gaussian potential this domain shrinks to a point resulting in disappearance of the enhanced densities in the center of the spike. Test-particle simulations of the electrons in the given potential indicate that the motion of the very low energy electrons can be well described by three harmonic oscillators with distinct frequencies for the parallel bounce and perpendicular gyration and drift. For higher energies the motion becomes deformed

3D - FatSW

step= 200 time= 40.00 el. charge(x,y) at z=8

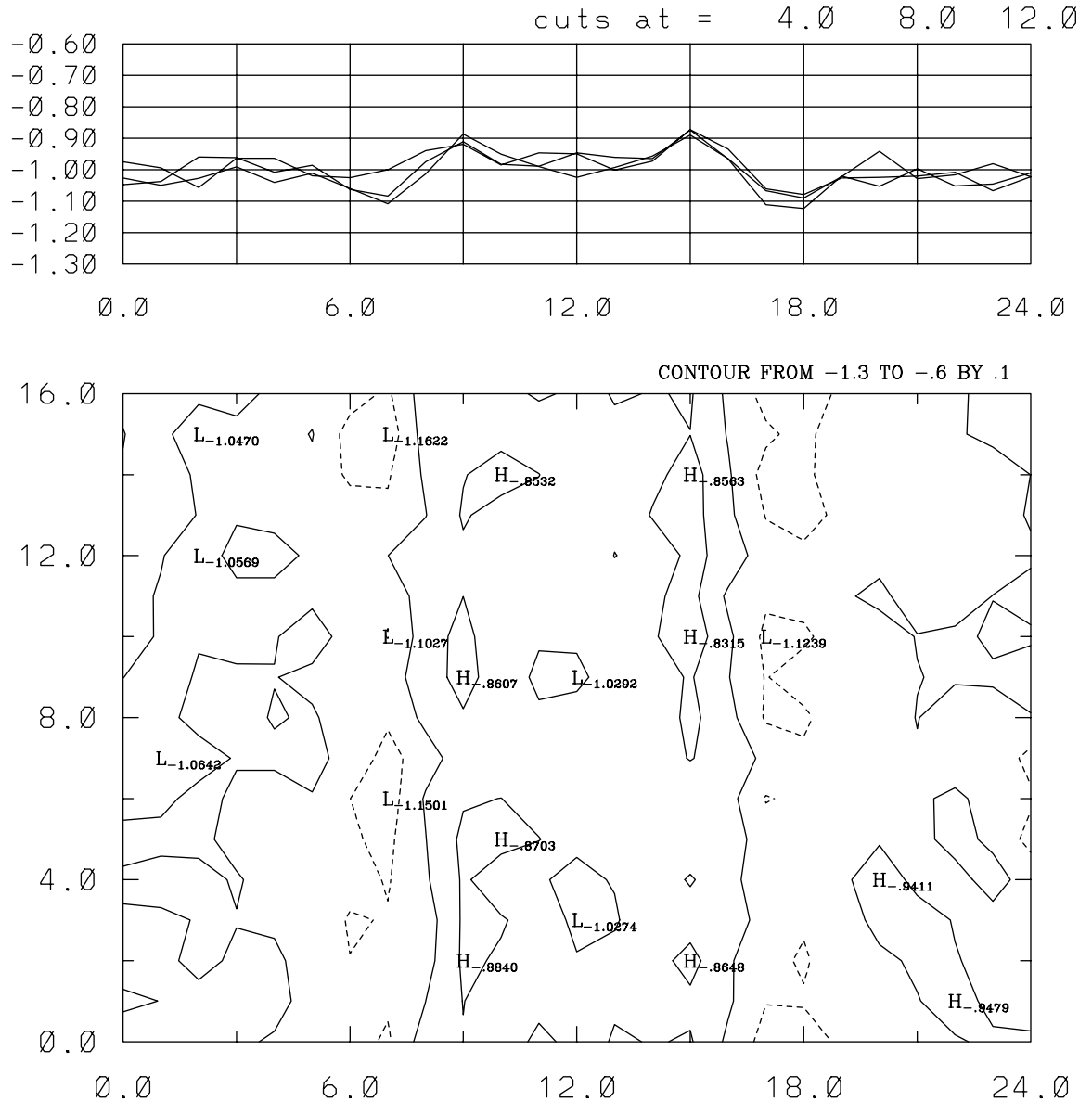


Figure 11. Potential projection $\phi(x, y)$ and cuts $\phi(x)$ at $z = L/2$ at the latest time of imposed approach of the secondary pulse. After that time a self-consistent interaction is allowed to take place.

owing to nonlinearity. However, owing to the relatively strong magnetization on the auroral field lines and the small perpendicular thermal spread, the gyroradius is much smaller than the perpendicular gradient scale length of the spike's potential. Thus the three eigenmodes of the electron dynamics are preserved, and only weak coupling between parallel and perpendicular oscillations occurs. The stability of a solitary structure depends on the adjustment of the trapped population to perturbations and to externally modified parameters. It is affected by the interaction with the impinging particles, by the changes in external conditions along the trajectory of the solitary structure, and by the resonant interaction between the trapped, supporting elec-

trons and additional wave eigenmodes. However, the strongest perturbations that affect the solitary structures are due to interaction with other spikes which move relative to the analyzed spike. When two spikes approach each other, the supporting electron distributions intermingle and their mixture may cause destruction or deformation of the spike(s). In particular, electrons around the separatrix exhibit significantly deformed trajectories. In the presence of a second spike approaching the primary solitary structure to a distance of the order of the scale length of the spike's electric field, some electrons from the primary structure diffuse into the secondary, smaller one. This net influx of electrons into the smaller spike dislocates the balance of the trapped, self-

3D - BGK spike

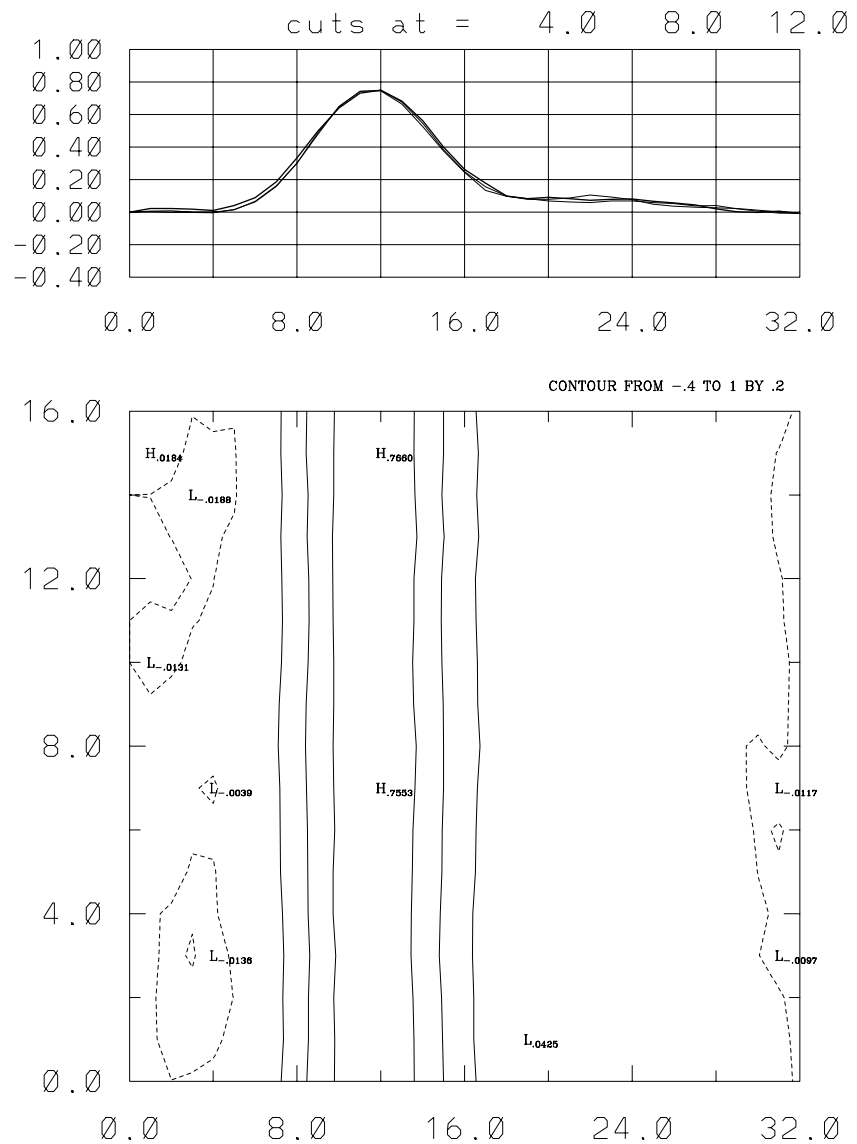
step= 300 time= 60.00 potential(x,z) at $y=L/2$ 

Figure 12. Two-dimensional projection of the potential $\phi(x, z)$ for $y = L/2$ and cuts $\phi(x)$ for three z values after the two spikes interact. One observes the disappearance of the smaller spike and average motion of the main structure in the original direction of the secondary spike.

consistent population which causes the perturbing spike to collapse. Since the secondary spike is much less intense than the primary solitary structure, its effect on the primary spike is small. Self-consistent particle simulations with open boundary conditions confirm the “cannibalizing” of the secondary spike, while the primary spike acquires momentum due to the loss of its separatrix electrons. These electrons penetrate the other spike and, with its disappearance, eventually become untrapped. Since they carry a nonnegligible amount of momentum, the primary spike receives a boost in the opposite direction. Similar conclusions have been drawn previously from entropy arguments. Therefore the interactions between spikes of different amplitudes is a source of redistribution of momentum between the

auroral solitary structures. The robustness of the nonlinear solitary structure in three dimensions explains their frequent observation by field crossing satellites. Although spikes undergo deformations and collisions because of a spread of their speeds along the field lines, these results from the test particle and the self-consistent simulations indicate that they are stable and long-living. However, emission of whistler-like waves may play an important role in their long-term evolution. Several outstanding questions relevant to the evolution of the auroral solitary structures include (1) the effect of the perpendicular field on the interaction of the spikes, particularly when the perpendicular drifts of the supporting electrons in both spikes are significantly different and their merging can affect additionally the collapse of the

3D - BGK spike

step= 525 time= 105.00 potential(x,z) at y=L/2

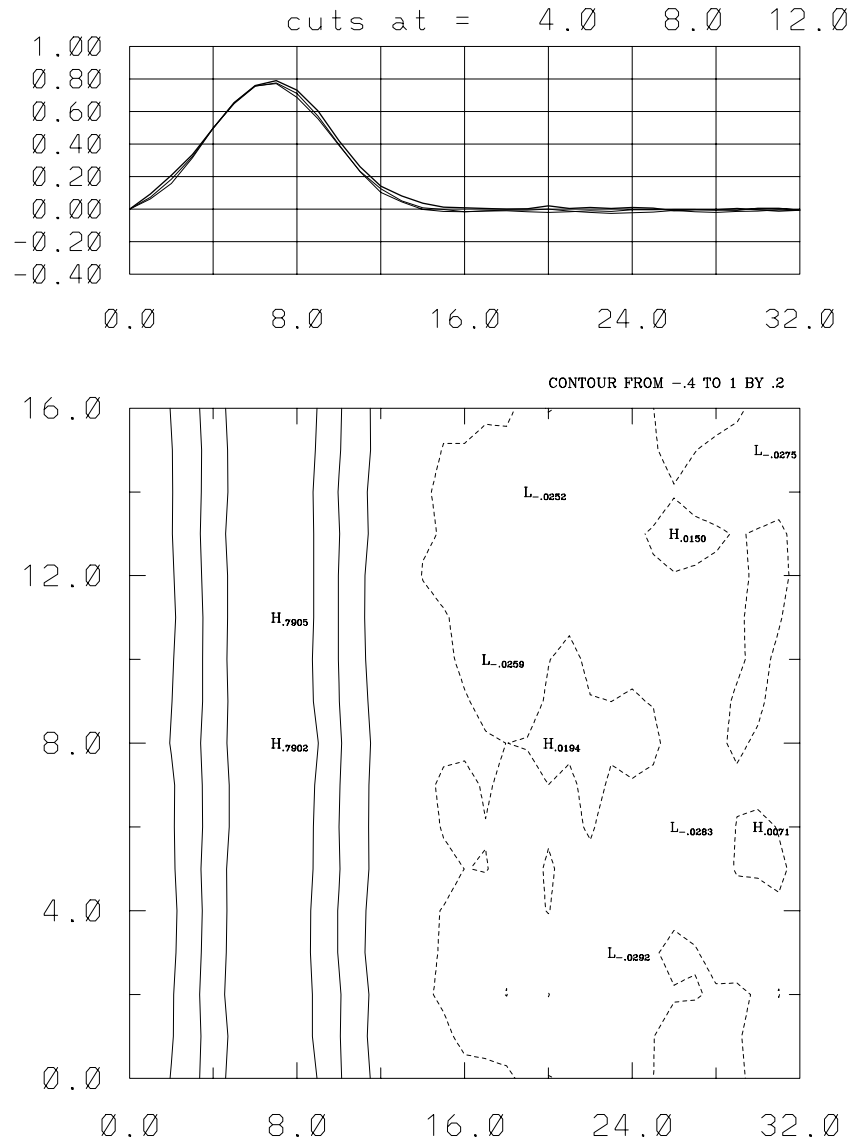


Figure 13. Two-dimensional projection of the potential $\phi(x, z)$ for $y = L/2$ and cuts $\phi(x)$ for three z values after the two spikes interact. The solitary structure continues to move self-consistently in the original direction of the secondary spike.

secondary spike, (2) the effect of the solitary structure on the ions due to the perpendicular field with the flat-top potential, which allows longer residence time of the ion in the spike and resulting enhanced heating, and (3) formation of the flat-top potential structures due to self-consistent interactions.

[7] **Acknowledgments.** We acknowledge the support of the grants NAG5-8078, NAG5-3596, and NAG5-3916.

[8] Hiroshi Matsumoto thanks M. Oppenheim and N. Singh for their assistance in evaluating this paper.

References

- Bale, S. D., P. J. Kellogg, D. E. Larson, R. P. Lin, K. Goetz, and R. P. Lepping, Bipolar electrostatic structures in the shock transition region: Evidence of electron phase space holes, *Geophys. Res. Lett.*, 25, 2929, 1998.
- Berman, R. H., D. J. Tetreault, and T. H. Dupree, Observation of self-binding turbulent fluctuations in simulation plasma and their relevance to plasma kinetic theories, *Phys. Fluids*, 26, 2437, 1983.
- Berman, R. H., D. J. Tetreault, and T. H. Dupree, Simulation of phase space hole growth and the development of intermittent plasma turbulence, *Phys. Fluids*, 28, 155, 1985.
- Bounds, S. R., R. F. Pfaff, S. F. Knowlton, F. S. Mozer, M. A. Temerin, and C. A. Kletzing, Solitary potential structures associated with ion and electron beams near $1R_E$ altitude, *J. Geophys. Res.*, 104, 28,709, 1999.
- Carlson, C. W., et al., FAST observations in the downward auroral current region: Energetic upgoing electron beams, parallel potential drops, and ion heating, *Geophys. Res. Lett.*, 25, 2017, 1998.
- Cattell, C. A., et al., Comparisons of Polar satellite observations of solitary wave velocities in the plasma sheet boundary and the high-altitude cusp to those in the auroral zone, *Geophys. Res. Lett.*, 26, 425, 1999.
- Crumley, J. P., C. A. Cattell, R. L. Lysak, and J. P. Dombek, Studies of ion solitary waves using simulations including hydrogen and oxygen beams, *J. Geophys. Res.*, 106, 6007, 2001.

- Dupree, T. H., Theory of phase-space density holes, *Phys. Fluids*, 25, 277, 1982.
- Ergun, R. E., et al., FAST satellite observations of large-amplitude solitary structures, *Geophys. Res. Lett.*, 25, 2041, 1998.
- Franz, J. R., P. M. Kintner, and J. S. Pickett, Polar observations of coherent electric field structures, *Geophys. Res. Lett.*, 25, 1277, 1998.
- Franz, J. R., P. M. Kintner, C. E. Seyler, J. S. Pickett, and J. D. Scudder, On the perpendicular scale of electron phase space holes, *Geophys. Res. Lett.*, 27, 169, 2000.
- Goldman, M., M. M. Oppenheim, and D. L. Newman, Nonlinear two-stream instabilities as an explanation for auroral bipolar wave structures, *Geophys. Res. Lett.*, 26, 1821, 1999.
- Krasovsky, V. L., H. Matsumoto, and Y. Omura, BGK analysis of electrostatic solitary waves observed with Geotail, *J. Geophys. Res.*, 102, 22,131, 1997.
- Matsumoto, H., H. Kojima, T. Miyake, Y. Omura, M. Okada, I. Nagano, and M. Tsutsui, Electrostatic solitary waves (ESW) in the magnetotail: BEN wave forms observed by Geotail, *Geophys. Res. Lett.*, 21, 2915, 1994.
- Miyake, T., Y. Omura, H. Matsumoto, and H. Kojima, Two-dimensional computer simulations of electrostatic solitary waves observed by the Geotail spacecraft, *J. Geophys. Res.*, 103, 11,841, 1998.
- Miyake, T., Y. Omura, and H. Matsumoto, Electrostatic particle simulations of solitary waves in the auroral region, *J. Geophys. Res.*, 105, 23,239, 2000.
- Morse, R. L., and C. W. Nielson, One, 2-, and 3-dimensional numerical simulation of 2-beam plasmas, *Phys. Rev. Lett.*, 23, 1087, 1969.
- Mozer, F. S., R. E. Ergun, M. Temerin, C. Cattell, J. Dombek, and J. Wygant, New features in time domain electric field structures in the auroral acceleration region, *Phys. Rev. Lett.*, 79, 1281, 1997.
- Muschietti, L., R. E. Ergun, I. Roth, and C. W. Carlson, Phase-space electron holes along magnetic field lines, *Geophys. Res. Lett.*, 26, 1093, 1999.
- Muschietti, L., I. Roth, C. W. Carlson, and R. E. Ergun, A transverse instability of magnetized electron holes, *Phys. Res. Lett.*, 85, 94, 2000.
- Muschietti, L., I. Roth, C. W. Carlson, and M. Berthomier, Modeling stretched solitary waves along magnetic field lines, *Nonlinear Processes Geophys.*, in press, 2002.
- Omura, Y., H. Matsumoto, T. Miyake, and H. Kojima, Electron beam instabilities as generation mechanism of electrostatic solitary waves in the magnetotail, *J. Geophys. Res.*, 101, 2085, 1996.
- Oppenheim, M. M., M. V. Goldman, and D. L. Newman, Evolution of electron phase-space holes in a 2-d magnetized plasma, *Phys. Rev. Lett.*, 83, 2344, 1999.
- Oppenheim, M. M., G. Vetoulis, D. L. Newman, and M. V. Goldman, Evolution of electron phase-space holes in 3D, *Geophys. Res. Lett.*, 28, 1891, 2001.
- Schamel, H., Kinetic theory of phase space vortices and double layers, *Phys. Scr. T*, 2/1, 228, 1982.
- Singh, N., and R. W. Schunk, Collisionless electron shock in electron-beam-plasma systems, *Phys. Fluids*, 26, 2781, 1983.
- Singh, N., and R. W. Schunk, Plasma response to the injection of an electron beam, *Plasma Phys. Controlled Fusion*, 26, 859, 1984.
- Singh, N., S. M. Loo, B. E. Wells, and C. Deverapalli, Three-dimensional structure of electron holes driven by an electron beam, *Geophys. Res. Lett.*, 27, 2469, 2000.
- Singh, N., S. M. Loo, and B. E. Wells, Electron hole as an antenna radiating plasma waves, *Geophys. Res. Lett.*, 28, 1371, 2001.
- Turikov, V. A., Electron phase-space holes as localized BGK solutions, *Phys. Scr.*, 30, 73, 1984.
- Vetoulis, G., and M. Oppenheim, Electrostatic mode excitation in electron holes due to wave bounce resonances, *Phys. Rev. Lett.*, 86, 1235, 2001.

C. W. Carlson, F. S. Mozer, L. Muschietti, and I. Roth, Space Sciences Laboratory, University of California, Berkeley, CA 94720, USA. (ilan@sunspot.ssl.berkeley.edu)

R. E. Ergun, Laboratory for Atmospheric and Space Physics, University of Colorado, Boulder, CO 80303, USA.

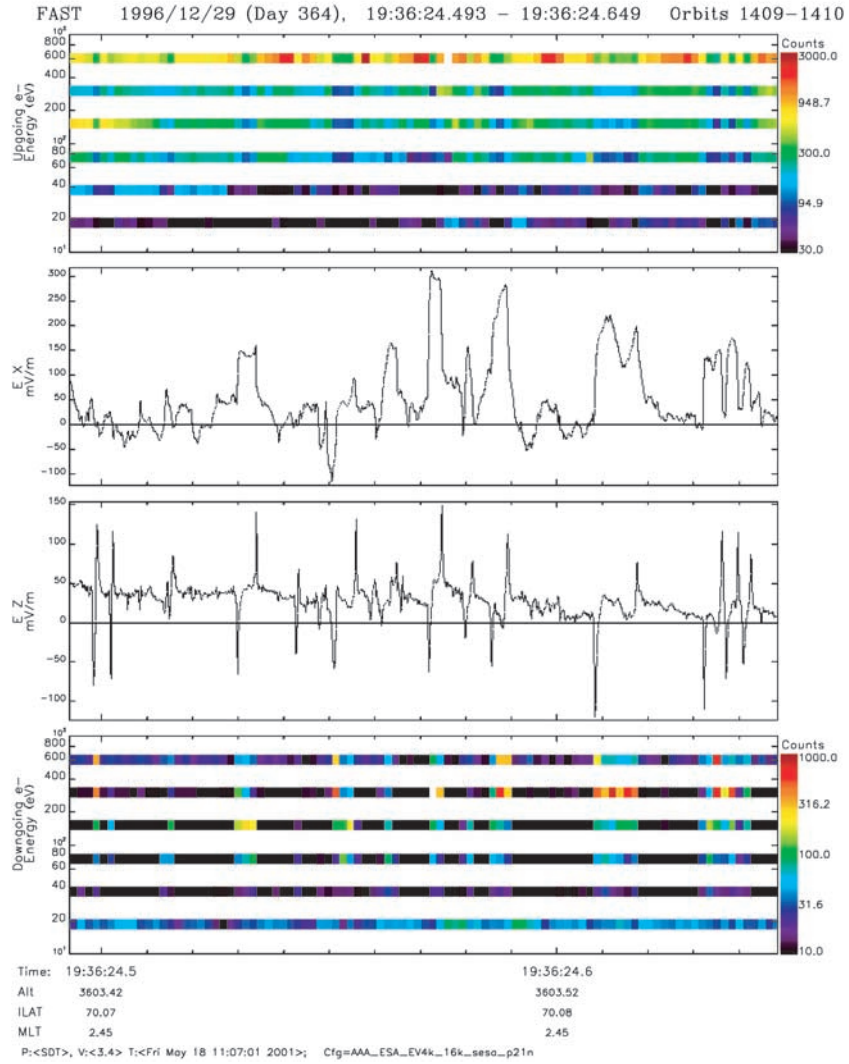


Figure 1. Energy fluxes at several energy channels for (top) upgoing and (bottom) downgoing electrons. (middle, top) Perpendicular and (middle, bottom) parallel electric field components with flat-top and Gaussian solitary structures.